Asummary of the Paper:

"Improving the recovery of monthly regional water storage using one year simulated observations of two pairs of GRACE-type satellite gravimetry constellation"

Basem Elsaka[1,3], Ehsan Forootan[2] and Abdulaziz Alothman[1]

1- Space and Aviation Research Institute, King Abdulaziz City for Science and Technology (KACST), Riyadh, Saudi Arabia
2- Institute of Geodesy and Geoinformation (IGG), University of Bonn, Germany
3- National Research Institute of Astronomy and Geophysics (NRIAG), Helwan, Cairo, Egypt.

Corresponding Author:

Dr. Basem Elsaka,
Corresponding Author's Institution: Space and Aviation Research Institute, King Abdulaziz City for Science and Technology

P.O.Box 6086, Riyadh 11442, Saudi Arabia,
 Tel: +966 503805697 | Fax: +966 114814572

Abstract

Increasing the spatial sampling isotropy is a major issue in designing future missions dedicated to continue the task of the Gravity Recovery And Climate Experiment (GRACE) mission. From various possible future satellite gravimetry scenarios, the two-pair multi-orbit satellite configuration (Bender-type in the sequence), consisting of a coupled semi-polar pair (the same as GRACE) and an inclined pair of satellites seems to be an optimal mission choice.

This contribution examines the performance of a Bender-type scenario at altitudes of 335 km and 352 km and inclinations of 89º and 63º, respectively, for improving the regional recovery of hydrological signals. To this end, we created one full year of simulated observations of the GRACE and Bender-type configurations. Our investigations include: 1) evaluating the feasible spatial resolution for recovery of terrestrial water storage (TWS) changes in the presence of realistic instrumental noise and errors in the background models; 2) assessing the influence of aliasing errors in the TWS recovery and its separation from instrumental noise and introduced hydrological signals; and 3) analyzing the regional quality of the gravity-derived TWS results by assessing water storage changes over the 33 world major river basins.

From our simulations, the Bender-derived spectral error curves indicate that, in spite of the instrumental noise, aliasing errors still contaminate the gravity fields above geopotential spherical harmonic coefficients (SHC) degree and order (d/o) 80 till 100. Regarding to the TWS recovery, we found notable improvements for the Bender-type configuration results in medium and small-scale basins, such as the Brahmaputra, Euphrates, Ganges, Indus, Mekong basins in Asia and the Yellow and Orange basins in South Africa. These results were achieved without applying post-processing, which was unachievable using simulations of one pair of GRACE-like configuration. Comparing the magnitudes of errors in the Bender-derived solutions with those of GRACE indicate that the accuracy derived from the Bender-type fields is about two times better than that of GRACE, specifically at medium spatial resolutions of 250 km (SHC d/o 80). We truncated the TWS recovery up to SHC d/o 80 in the spectral domain, whereas all comparisons are demonstrated in the spatial domain after a truncation of the solutions and WGHM field at d/o 60, since beyond this range; a relatively strong instrumental and aliasing errors contaminate the solutions.

Our numerical results indicate that the spatial resolution of the Bender-type TWS recovery can be even higher for the basins with strong temporal water storage variations such as the Amazon basin. Short wavelength mass variations in basins with relatively weaker temporal TWS magnitude, such as the Murray basin, might still need the application of a filter with small averaging kernel.

Keywords. Regional water storage, Gravity recovery, Temporal aliasing, Bender constellation.

1. Introduction

Time-variable gravity field solutions derived from the Gravity Recovery And Climate Experiment (GRACE) have already provided valuable information about the global water storage variations with an accuracy of few centimeters at scales of a few hundred kilometers and larger (e.g. Tapley et al., 2004, Kusche et al., 2012). This time series has been provided by various GRACE analysis centers such as UTCSR (University of Texas Center for Space Research, Tapley et al., 2005), GFZ (German Research Center for Geosciences; EIGEN models; Dahle et al. 2013) or the University of Bonn (ITG-GRACE series; Mayer-Gürr et al., 2010). None of the solutions, however, has met the predicted pre-mission accuracy of GRACE that was derived by Kim (2000). The factors that limit the GRACE accuracy include not only instrument and system noise (Sheard et al. 2012), but also temporal aliasing errors (Flechtner et al., 2010, Forootan et al., 2013,2014a) and anisotropy of the spatial sampling due to the GRACE orbital design (Sneeuw et al., 2004).

In the following, the introductory section is arranged in three main parts. The first part addresses the instrumental noise in addition to the type of aliasing (temporal and spatial) that affects the gravity field solution. The second part focuses on improving the spatial isotropy in the context of designing future satellite gravimetry missions through the recent studies, especially that related results in Wiese et al (2011). The third part discusses the recovery of total water storage (TWS) changes as a main product of satellite gravimetry missions. At the end of the introductory section, the scope as well as the organization of this paper is presented.

The instrument and system errors can be significantly reduced when the K-band inter-satellite ranging (KBR) system of the current GRACE mission is replaced by a laser ranging interferometer (LRI), which will be tested for the first time as a secondary payload on GRACE-FO (Follow-on) in August 2017 (Flechtner et al. 2014). The future LRI ranging precision is projected to exceed hundreds times the GRACE KBR micrometer level (see e.g. Pierce et al. 2008 and Sheard et al. 2012). The second issue, the aliasing problem, consists of two main parts, i.e. the spatial and temporal aliasing. Spatial aliasing occurs as a result of truncating the true mass signal (e.g. caused by hydrological variability in our case) at a certain degree and order (d/o) of the spherical harmonic representation. For instance, assume that the simulated 'true' hydrological signal, which itself simplifies the real world by modeled values, contains water storage information represented by spherical harmonic coefficients (SHC) of d/o $2 < N_{max} < 100$ (this is the case for the WaterGap Hydrological Model (WGHM, Döll et al. 2003) used in this study). If the recovered hydrological solution from GRACE gravity field modeling contains signals only up to d/o $N_{max}= 40$, the short wavelength spatial hydrological variability corresponding to d/o $41 < N_{max} < 100$ will be spatially aliased into the GRACE monthly solutions.

Temporal aliasing occurs due to the temporal under sampling of GRACE monthly observation intervals. As a result, high frequency short-term (hours to days) mass variations in the ocean, atmosphere and land hydrology might be aliased into lower frequencies, thus, contaminating GRACE monthly 'mean' hydrological signals. For example, imperfect reduction of the

atmospheric and oceanic de-aliasing products is addressed as an issue that introduce errors in mass estimations from GRACE monthly products (Flechtner et al., 2010, Forootan et al., 2014a).

Increasing the spatial isotropy of gravity sampling, possibly to a level that doesn't require the use of post-processing techniques, such as filtering, has been discussed in the context of designing future satellite gravimetry missions. The goal can be achieved, for instance, by adding another satellite pair to the current semi-polar orbit GRACE design in a polar or an inclined orbit (see e.g. Bender et al., 2008, Visser et al., 2010, Wiese et al., 2011, NGGM Team, 2011, NG2 Team, 2011, Wiese et al., 2012, Elsaka 2014a and Elsaka et al., 2014). We should also mention that a number of other configuration options have been investigated in the last years (e.g. Sharifi et al. 2007, Sneeuw et al. 2008, Wiese et al. 2009, Elsaka 2010 and Iran-Pour et al. 2013). These studies compared the performance of alternative single pair satellite formations (e.g. pendulum, Cartwheel or LISA-type) and found that the latter three missions would provide a lower error spectrum with improved isotropy. As a result, such satellite formations potentially provide reduced level of the "striping" behavior associated with the time-variable gravity solutions, compared to those derived from the GRACE mission configuration. In fact, using multiple satellite pairs, the large equatorial ground track spacing of polar orbits can be reduced, and hence, a higher isotropy due to the larger intersection angles of the ground tracks with the meridians can be achieved. However, the mission costs will rise if more satellite pairs are flown, in particular if different inclinations are desired different launchers will become necessary. From the proposed satellite formations, parallel flights of two GRACE-type missions derived, e.g., by combining one single pair of GRACE-type twins in a polar orbit with another pair flying in a relatively lower inclination of 63° as proposed by Bender et al. (2008), seems to be technically feasible (see also NG2 Team, 2011, Elsaka et al. 2014).

Wiese et al. (2011) reported improvements in the TWS recovery by considering a Bender-type configuration in an improved temporal sampling of 13-day repeating orbits. However, the selected 13-day repeating mode is still not sufficient for reaching the desired improvement in high frequency signals with e.g. daily resolution. Reaching to the high temporal resolution, e.g., daily, will be at the cost of losing the spatial resolution, especially around equators (around 2600 km resolution), where consideration of tropical water storage signals is desired. One might conclude here that observing short temporal mass variability is hardly achievable via satellite gravity missions due to their high costs, since many satellite pairs will be required to be launched in a number of maneuvers. Instead, using a combination of models and observations, one could achieve the desired daily temporal resolution. This has been done, for instance, in Kurtenbach et al. (2009, 2011) who combined available ocean, hydrology and atmospheric models with GRACE satellite gravimetry observations to produce daily ITG-Kalman gravity field products.

It should be mentioned here that a trade-off in selection of a repeat mode always exists. In other words, for instance a 13-day repeat orbit e.g. in Wiese et al. (2011) or a 30-day period in the current study, are not the final or the optimum decision. This selection depends mainly on what the science goals of the mission are. In fact, considering a longer repeat period does not always

guarantee superior spatial resolution since temporal aliasing errors accumulate over the longer periods and can further degrade the accuracy of the solutions compared to shorter repeat periods. To prove this we refer here to Wiese et al. (2009), who used 30-days of satellite observations of two- and four-satellite cartwheel formations. In their study, it was found that unlike the noise-only cases, the aliasing results show that the two- and four-satellite GRACE and Cartwheel formations determine the gravity field fairly equal in the presence of aliasing (i.e. no obvious improvement was obtained).

Time-variable terrestrial water storage (TWS) (the sum of groundwater, soil moisture, surface water, and snow) maps are the main products of satellite gravimetry missions (Tapley et al., 2004). However, the spatial resolution of GRACE-derived TWS changes is low compared to the hydrological models (Rodell et al., 2004). Besides, the GRACE-derived gravity solutions at higher degrees are too strongly affected by correlated noise (e.g., Kusche, 2007). Within simulations, we will show that the GRACE-derived potential coefficients of higher than degree 25 are affected by both instrumental and aliasing noise. This is confirmed by other simulation studies, e.g., Han et al. (2004), and the analysis of real GRACE data e.g., (Schmidt et al. 2008). Smoothing the GRACE-derived mass results, and/or averaging over specific regions, thus, needs to be applied to GRACE-derived TWS fields. This issue is usually discussed in the context of filtering approaches (see e.g., Swenson and Wahr, 2006, Kusche, 2007, Klees et al., 2008). As a result of applying both smoothing and averaging operators, within filters, some mass anomalies are displaced, which causes biases in the mass change estimations over areas of interest, e.g., lake and river basins. This problem is referred as the 'leakage' problem in e.g., (Swenson and Wahr, 2002, Klees et al., 2007). Spatial leakage prevents GRACE data to be used to their full information extent, and subsequently, a leakage reduction approach must be used to reduce the impact and derive unbiased mass estimations (Fenoglio-Marc et al., 2006, 2012, Longuevergne et al., 2010, Forootan et al., 2014b). Therefore, estimating accurate mass variations with high spatial resolutions, over the land, might offer more opportunities to improve their water variation investigations or hydrological models (Eicker et al., 2014). Jensen et al (2013) pointed to an inconsistency between GRACE results and modeling of water storage over major river basins, and consequently the quest for high resolution satellite-derived mass estimation and better modeling approaches. These examples motivated us to select monthly repeat orbits for the simulation of GRACE and Bender-type configurations in this study. This selection offers a sufficient spatial coverage, especially, to investigate all the 33 world's largest river basins (located between the latitudes $\pm$ 60º) without affecting the spatial homogeneity of gravity sampling (known as spatial coverage).

In this study, we will investigate three main issues related to the recovery of TWS signals, using satellite gravimetry observations. In (1), the recovery of temporal gravity fields at different spatial resolutions (half-wavelength) of 500 km, 250 and 200 km (corresponding to the geopotential SHC expansion of up to d/o 40, 80 and 100, respectively) is examined. Our motivation to perform this assessment is to understand at which spatial resolution one can extract more information about the hydrological signal considering the fact that both instrumental noise

and aliasing effects (here introduced as background model differences) would be accumulated at high degree and order coefficients (see Han et al., 2004, Elsaka et al., 2014). In (2), the behavior of the aliasing errors in the recovery of TWS changes and its separation from instrumental noise and the introduced monthly TWS signals is assessed. This investigation identifies the benefits and limitations of using the multi-satellite Bender-type configuration in order to decrease the aliasing errors. In (3), the recovery of seasonality and trend of TWS changes over the 33 world major river basins has been assessed. This investigation has been performed both in terms of basin averages as well as spatio-temporal variability. Thus our assessment in (3) will provide examples of comparisons between the introduced 'true' TWS changes and their regional recovery, while considering different water storage magnitude and water distribution within the assessed basins.

This contribution is organized as follows: In section 2, we describe our simulation scenarios. Then the tests regarding the recovery of TWS changes in both global and regional scales are presented in section 3. Finally, some conclusions relevant for the analysis of TWS signals from the observations of a Bender-type mission are provided in section 4.

2. Simulation strategy

The simulated observations for the Bender-type satellite configuration as well as the GRACE mission (used for comparisons) is based on orbital geometry given in Elsaka et al. (2014), where a variety of orbit parameters including the orbital altitude, the inter-satellite distance, the inclination, the repeat mode, as well as the choice of the number of satellites and satellite links were investigated. The simulated GRACE scenario here adopts the details of the real GRACE mission with an orbital inclination of 89º, an 'initial' orbital height of 460 km, and the inter-satellite range of 220 km. The Bender-type multi-orbit satellite configuration, here, consists of a polar satellite pair (Bender 1&2) coupled with a lower inclined (63°) satellite pair (Bender 3&4) flying in orbital heights of 335 km and 352 km, respectively, each of which has an inter-satellite range of 100 km. Satellite ground tracks of both simulated GRACE and Bender-type configurations are shown in Fig. 1. Obviously, more homogenous and dense spatial coverage was derived from our Bender-type simulations. The lower orbital height of the Bender-type configuration, when compared to GRACE, increases the signal-to-noise ratio and hence provides significant improvements (see Elsaka 2010, pp. 59). Nevertheless, the GRACE's inter-satellite distance, when compared to that of the Bender-type, provides also significant improvements (see Elsaka 2010, pp. 62). We should mention that a comparison of one-pair of satellites at the same orbital altitude and with the same measurement noise as that of the Bender-type configuration has been performed by Elsaka (2014b). In his study, it was found that the latter configuration provides about one full order of magnitude better than that of GRACE-type. However, we keep in this study the performed comparisons, since the focus of the paper is to investigate the possible improvements of total water storage recovery using a modern gravimetry mission, rather than only a fair comparison (i.e. same altitude and inter-satellite distance) with the GRACE configuration.

The numerical simulation is performed by integrating sequentially the satellite orbits of each formation over a time span of one full year, while applying true background models as indicated in Table 1. The simulations are performed to recover the monthly continental TWS changes in the presence of modeling errors (see Table 1), as well as measurement system errors based on Elsaka et al. (2012), where measurement noise was added to the error-free observations by using a random Gaussian noise generator with a standard deviation equal to 1 cm in position for all three directional components of both GRACE and Bender-type formations, as well as a Gaussian noise in range-rate of micrometer level (0.5 μm/s) for GRACE and nanometer level (50 nm/s) for Bender. The numerical simulation procedure applied in this paper is identical to that described by Elsaka et al. (2012), where the majority of the details were illustrated.

Figure 1

The reason for selecting the measurement noise based on Elsaka et al. (2012) is that, the simulated "noise-only" GRACE solution meets the expectation of the pre-launched mission accuracy (i.e. to the GRACE baseline as shown in Fig. 2). Therefore in our case, we run this scenario in order to compare the accuracy levels that are determined from the future gravity mission with an 'optimistic' GRACE accuracy. In other words, the simulated scenario might be closer to the accuracy of GRACE Follow-On (GRACE-FO) mission, scheduled for launch in 2017 (Flechtner et al., 2014), which still adopts the GRACE design of two satellites flying in one orbital plane, and at the same time a more accurate laser instrument has been used to measure inter-satellite distance. We should also mention here that choosing higher noise level of K-band range-rate may lead to a significantly worse impact on the gravity solution than the impact of the temporal variation itself. For instance, Visser et al. (2010) applied two different low-low satellite-to-satellite tracking (ll-SST) noise levels, i.e. 1.0 and 0.01 μm/s. The noise level of 1.0 μm/s is rather conservative considering the GRACE performance according to Frommknecht et al. (2006), whereas the 0.01 μm/s is considered feasible with future laser-based sensor systems according to Thales Alenia Space (2008). Visser et al. (2010) then reported that applying ll-SST (low-low satellite-to-satellite measurement) noise level of 1.0 μm/s leads to dominant errors larger than the simulated temporal (tide in their case) model differences, whereas the temporal differences are seen clearly when the noise level was selected more optimistic to be 0.01 μm/s (see also Elsaka (2010), pp. 93, who confirms a similar finding).

We should mention here that the Bender-type configuration is assumed here to be a drag-free mission. This means that the accelerometer observations were set as zeros for this configuration. However, simulated accelerometer noise of 1×10^{-10} m/s^2 magnitude was considered as the noise level of this assumption. For the GRACE mission, the acceleration noise level of 9.8×10^{-9} m/s^2 was applied as given in Elsaka et al. (2014).

Finally, in order to identify a 'realistic' aliasing impact on the recovered gravity solution, we ran orbit integration due to the time-variable ocean tides, as well as the atmospheric and oceanic de-aliasing (AOD) models, to introduce variability (see Table 1) along the GRACE and Bender-type orbits (caused by introducing monthly terrestrial water storage (TWS) signal from WGHM

(WaterGap Global Hydrological Model, Döll et al., 2003) over the full year of 2006. To estimate the monthly geopotential SHCs, errors in the ocean tides and AOD models (see Table 1) in the presence of the mentioned measurement noise were applied to each month of year 2006 during the setup of observation equations, required for recovery of monthly hydrological signals. It is important to address here that, the name of "noise-only" scenario (see Table 1 and Fig. 2) was chosen to emphasize that we recover TWS changes based on noisy measurements. This scenario, however, contains in reality aliasing errors, since we recover monthly mean of WGHM in the gravity analysis step, whereas, daily WGHM was applied during the orbit integration step. In the "noise +aliasing" scenario, the aforementioned errors in tides and AOD models in addition to the measurement noise were considered during the recovery of the monthly mean of WGHM-TWS.

Since our study considers the recovery of TWS from the Bender-type configuration at different SHD resolution of 40, 80 and 100, the introduced mean 'static' gravity field as well as background models (Table 1) have also been correspondingly truncated in the orbit integration step to coincide with the recovery step. This is done in order to distinguish between the noise-only and the noise + aliasing cases (see section 3) without the influence of the accumulated SHC of background models (beyond the truncation degree) on the observations.

Table 1

3. Computation tests for hydrology recovery

In the following sections, we present a number of test computations that address the global and regional TWS recovery through closed-loop simulations. At first, we briefly review the scientific requirements, which are desired for the TWS products from a future mission. Then, the performed numerical simulations and their results are presented.

3.1. Global hydrology recovery

To examine the effect of measurements noise only on the recovery of the temporal hydrological signal introduced by WGHM (Döll et al. 2003), numbers of test computations were performed. These include the recovery of TWS at different spatial resolutions of 500 km, 250 km and 200 km that respectively correspond to the gravity solutions expanded in spherical harmonics up to d/o 40, 80 and 100. Eq. [1] relates the maximum degree of gravity solutions to its corresponding spatial resolution at the equator as

$$N_{max} \approx \frac{2\pi R_E}{\lambda} \approx \frac{40.000}{\lambda} \approx \frac{20.000}{D}, \qquad\qquad [1]$$

where N_{max} is the maximum spherical harmonics degree (SHD), R_E is the mean radius of the Earth, λ is the wavelength in km, D is the resolution (half-wavelength) in km.

Other scenarios have also been run to examine the combined effect of instrument noise and the modeling differences (i.e. aliasing errors) on the recovery of TWS changes. Fig. 2 summarizes the results of our simulation scenarios in both mentioned cases, in which noise-only stands for the

first scenario and noise + aliasing stands for the second scenario (see Table 1). The results are shown in terms of degree variances of geoid heights that have been often used to quantify the powers of signal and error in the gravity field estimates at various spatial wavelengths as

$$\Delta\sigma_n^2 = R_E \sum_{m=0}^{n} (\Delta c_{nm}^2 + \Delta s_{nm}^2), \qquad [2]$$

with Δc_{nm} and Δs_{nm} being the differences between the estimated 'recovered' gravity coefficients and the reference 'true' model as

$$\Delta c_{nm} = (c_{nm})_{recovered} - (c_{nm})_{reference},$$

$$\Delta s_{nm} = (s_{nm})_{recovered} - (s_{nm})_{reference}.$$

Figure 2

All the simulation scenarios, presented in this study, have been started with a 'zero baseline' closed loop simulation, where synthesis and recovery are demonstrated in an error-free situation (Fig. 2, dashed curves). After adding noise to the measurements (as indicated in Sec. 2) including those of precise orbit determination (POD), satellite-to-satellite (SST) range-rates, and accelerometer data (the latter are zeros when considering the Bender-type configuration), we analyzed the gravity field to examine the effect of the introduced noise level on the gravity recovery (see Fig. 2, the difference between dashed and solid 'both in red and green' curves). In addition, we have plotted the pre-launched GRACE baseline (simulated for two satellites chasing each other at 500 km altitude from the surface of the Earth) as a comparison. Fig. 2 indicates that the Bender solution (noise-only) represents better accuracy than the GRACE solution, whereas the accuracy derived from our Bender-type configuration was more than one full order of magnitude better than that of GRACE. This is evident particularly at medium-to-short spatial wave-length, i.e., SHD up to d/o 60 – 100. These improvements correspond to a geoid accuracy of better than 0.1 mm at d/o 100. This finding agrees with previous studies that address a similar range of accuracy (cf. Fig. 4 in Wiese et al. 2011 and cf. Fig. 4 in Elsaka et al. 2014).

From Fig. 2, one can also see that the error curves of GRACE (in red) intersect the curve corresponding to the introduced mean time-variable TWS signal around d/o 35 – 40 (see also Fig. 4), whereas that of Bender-type 'green' error curves intersect it around d/o 65 – 70 (see also Fig. 4). One can infer from this result that 'in an optimal case, i.e. without contamination of aliasing errors' the Bender-type configuration would be able to provide better spatial resolution without requiring application of a filtering approach. The much lower error magnitude, found in the error curve of the Bender-type solutions, is firstly due to the combination of two SST baselines, which increases the spatial sampling of the mission. Additionally, lower orbital height of both Bender pairs strengthens the recovery of the gravitational signal. Finally, using improved sensors (providing lower sensor noise) increases the signal-to-noise ratio, and hence, provides significant improvements in recovery of TWS changes.

9

Moreover, we provide here the covariance estimation of the solutions, which shows the full error information of the spherical harmonics provided by the GRACE and Bender-type configurations (Fig.3). The selected covariance matrix in Fig. 3 (top), computed following Mayer Gürr et al. (2010), indicates less expected errors from the Bender-type mission scenario. The lower magnitude of errors includes the whole SHC types of zonal, tesseral and sectorial. This can be additionally seen in Fig. 3 (middle), which shows the true errors (i.e. recovered spherical coefficients minus the reference ones, see Eq. 2). In Fig. 3 (bottom), the formal errors are given, which represent the diagonal elements of the covariance matrix. Comparing Fig. 3 (left panel) with Fig. 3 (right panel) indicates that the error structure of the Bender-type solution is homogenously distributed, especially in the long wavelengths. As seen in Figs. 2 and 3, the errors at high degrees (namely SHC of d/o 35-100 provided by the GRACE and SHC of d/o 55-100 provided by the Bender-type configuration) are dominantly contaminated with errors. Yet, we should identify, whether the errors are resulted from measurement noise or accumulated aliasing errors, which is addressed in the following.

Figure 3

To understand the error structure of the performed recovery process, we repeated our simulations and TWS recovery processes at different wavelength ranges (d/o 40, 80 and 100) corresponding to the spatial resolutions of 500 km, 250 km and 200 km, respectively. The difference between outcomes of these scenarios would help us to discriminate between errors due to measurement noise and temporal aliasing. Error curves in Fig. 2 indicate that the temporal aliasing errors affect the average recovery of the introduced TWS signals at all wavelength ranges. In Table 2, we report the root mean squares (RMS) of the noise-only (i.e. gravity field analysis with measurement noise) and noise + aliasing (i.e. gravity field analysis with measurement noise and temporal aliasing), simulations of GRACE and the Bender-type mission scenarios, both for January 2006. The results in Table 2 indicate that noise and aliasing errors significantly increase for the GRACE scenarios (compare d/o 80 and d/o 100 of GRACE noise + aliasing to those of noise-only). Smaller differences were, however, found for the Bender-type scenarios.

Table 2

The results in Table 2 can also be seen as an obvious deviation between both error curves of the noise-only case and the noise + aliasing case determined by the GRACE formation. This appears especially at SHD from d/o 25-30 up to d/o 80 (compare the error curves of green and orange circles) and at SHD from d/o 25-30 up to 100 (comparing the solid green and orange error curves). This deviation indicates that introducing aliasing noise together with instrumental noise worsens the accuracy of TWS changes derived from the GRACE scenario.

Regarding the Bender-type solutions, one can see slight differences between both noise-only and noise + aliasing cases at SHD from 43 up to d/o 55-60 (error curves of blue and purple circles), whereas noticeable differences can also be seen from d/o 55-60 up to d/o 80. The same finding holds also, when the maximum truncation degree was selected 100 instead of 80 (solid blue and purple error curves). The latter results indicate that the aliasing errors are not an issue for the Bender-type mission scenario up to d/o 55-60, and therefore, we are not in a demand for a post-processing below d/o 55-60. Beyond d/o 55/60 a filter with small averaging kernel (e.g. Gaussian with small radius) might need to be applied. In light of our results in Fig. 2, they indicate that the de-aliasing errors appear in all spectra of the recovered gravity products. The level of these errors is lower for low degree coefficients. Their magnitude becomes dominant in high degree coefficients. Therefore, improving the de-aliasing procedure seems to be urgent for modern satellite gravimetry missions.

To assess the robustness of the performed TWS recovery scenarios from both the GRACE and Bender-type configurations, we ran our simulated satellite observations during one full year 2006. The results in terms of degree variance of geoid heights are shown in Figs. 4 and 5. We believe that the presented results of the Bender-type simulation are robust, since within the designed simulations various attempts have been taken out to properly select the formation parameters (e.g. orbital altitudes, inclinations, and inter-satellite baselines), as well as the selected instrumental and background noise level. In the following, we will repeat the scenarios for a whole year of TWS changes, derived from daily simulations of WGHM, and represent the range of accuracy for different months of TWS recovery from the GRACE and Bender-type configurations. In all cases, TWS fields derived from the Bender-type simulation was almost 10 times better than that of GRACE, particularly at medium and short wavelengths.

From our results (Fig. 2), one can conclude that the aliasing errors are counted as the dominant source that affect the accuracy of the TWS recovery not only for the GRACE scenario (particularly from degree 25-30 up to higher SHD) but also it seems to be a main issue for the Bender-type mission (particularly from degree 55-60 up to higher SHD. From a different point of view, Forootan et al. (2013) came to the same conclusion that the quality of de-aliasing products might be revisited, to be better suited to a relatively more precise mission such as a Bender-type configuration.

In light of our results, described above, the significant contribution of the Bender-type configuration shows improved performance with respect to GRACE for all degrees beyond SH d/o 25 up to d/o 55 and 70, where the introduced TWS signals were clearly recovered without

significant contamination of errors. These results point to the same direction as Wiese et al. (2011), who also found that the significant contribution of the Bender-type mission scenario for the hydrology and ice mass recovery being around wavelength equivalent with d/o 45. However, they stated that regional signals still exist that can be detected without post-processing to degree/order 60, (truncation degree in Wiese et al., 2011). Therefore, we decided to restrict our monthly computations up to only d/o 80 (not d/o 100). This decision also accelerated the computational load of the performed simulations significantly.

Fig. 4 shows the results of gravity field solutions, corresponding to 12 months of 2006, in terms of degree variance of geoid heights. The simulations were done for both the GRACE and Bender-type mission scenarios, considering the noise-only case. The results show that the estimated error curves are consistent with the mission definitions. As it is clear from the curves, the derived errors represent a robust behavior with respect to the introduced hydrological signals, i.e. regardless to the strength of the introduced hydrological signal; the error curve of the Bender-type mission scenario at a spatial resolution of 285 km (corresponding to d/o 70) was reproduced. Thus, this finding confirms the validity of our assessment in Fig. 2.

 In Fig. 5, the results of TWS recovery from January till December of 2006 for both GRACE and Bender-type mission scenarios are shown. It can be seen in most of the curves that the Bender-type mission was able to detect the hydrological signal at a spatial resolution of 333 km (corresponding to d/o 60). This emphasizes the fact that the temporal aliasing errors represent a dominant contamination role at recovery of small wave-length monthly mass variations (mass anomalies of smaller than 333 km).

We should mention here that the derived results support the choice of our temporal recovery using 30-day repeating mode, with detecting the hydrological signal up to d/o 60, whereas Wiese et al 2011 (cf. Fig. 4) could recover up to only d/o 45 of the signal (hydrology + ice in their case) using the Bender-type configuration at 13-day repeating orbit.

So far, our comparisons only included the direct analysis of spectral power (through degree variances). To complete our assessments, we also investigated the hydrological recovery within the 33 world largest river basins. This investigation is motivated from the fact declared by Han and Ditmar (2008) that state the time-variable signals (such as hydrology) depends on a certain region and decay rapidly away from the region while satellite gravity data contain all other signals and errors outside the region of interest. Therefore, one should consider the local impacts of using a modernized mission in recovery of the hydrological signals which is described in the following.

Figure 4

Figure 5

3.2. Regional hydrology recovery

In this section, first we discuss the recovery of simulated basin mean water storage changes over the world 33 major river basins (Fig. 6). Then, the spatial patterns of introduced signals over the Amazon as well as both Murray and Eyre basins together (Murrary+Eyre) and their TWS-recovery are illustrated. Our motivation to select the latter basins is due to their different signal contents. Amazon is known by its strong seasonal signal, while Murrary+Eyre exhibit relatively weaker temporal hydrological variability (Awange et al., 2011).

Fig. 7 shows the difference between recovered water storage signals determined by the Bender-type and the GRACE minus the simulated 'true' signal of WGHM, corresponding to the 33 world major river basins. The time series of Fig. 7 are in terms of basin averaged equivalent water height over 12 months of the year 2006. To have a fair comparison, the three water storage products were truncated at d/o 60. The basin averages were computed in the spectral domain (see e.g., Kusche et al., 2011), while no filtering was applied on the three products. The black curves in Fig. 7 represent the differences between Bender-type TWS recovery and WGHM and the blue curves represent those of GRACE-recovery and WGHM. Note that the high magnitude of the differences is due to the fact that the introduced WGHM signals have a spatial resolution of ~ 225 km (SHC 80) and the estimated basin averages are up to SHC 60. Therefore, the presented differences also contain spatial aliasing errors that make our comparisons close to the real case.

As expected, better regional recovery was achieved from the Bender-type configuration in most of the basins (i.e. differences close to zero). Therefore, the results include not only the largest river basins (meant here for those basins larger than 1,000,000 km^2) such as Amazon and Parana in south America, Lena, Ganges, Indus, Yangtze and Yellow in Asia, Niger and Nil in Africa, Murrary in Australia and Mississippi in north America, but also for those of medium (i.e. between 1,000,000 km^2 and 500,000 km^2, such as Orange in Africa, Mekong in Asia and Danube in Europa) and smaller (i.e. smaller than 500,000 km^2, such as Dnieper in Europa) spatial scales. Considering the variance of the introduced hydrological signals, and those of recovery, we observed that those recovered by the Bender-type mission reproduce about 80% – 90% of the introduced TWS variances. Examples include the TWS recovery of the basins in Asia, including Brahmaputra, Euphrates, Ganges, Indus, Mekong, as well as Yellow and Orange in South Africa.

Besides the improvement in estimation of basin average TWS changes, spatial resolution of the satellite gravimetry-derived water storage products is important for various hydrological applications. Examples include those applications, which try to assimilate satellite-derived water storage changes in hydrological models (e.g., Houborg et al., 2012, Eicker et al., 2014, Schumacher et al., 2014), or those who use the satellite products for monitoring (e.g., Awange et al., 2013). In Figs. 8 and 9, we compare the recovery of TWS over the Amazon and Murrary+Eyre basins with the introduced signal of WGHM, respectively. Similar to Fig. 7, all the comparisons are performed after a truncation of the solutions and WGHM field at d/o 60. This

was selected since beyond this range; a relatively strong instrumental and aliasing errors contaminate the solutions (as it was demonstrated in Fig. 5).

As it was seen in Fig. 7, the accuracy of recovery of Bender- and GRACE-derive basin averaged TWS changes over the two Amazon and Murrary+Eyre basins were quite similar. The spatial patterns in Fig. 8, however, indicate that the Bender-type solutions represent similar pattern as the originally introduced water storage patterns (from WGHM). The GRACE-like solutions hoever were found distorted with the north-south striping patterns. The same holds for the Murrary+Eyre basins, in which the amplitude of the striping pattern is almost as strong as the GRACE-derived TWS variations. Such distortion necessitates the application of a filtering approach to reduce the noise (e.g. Kusche et al., 2009). From the results in Figs. 8 and 9 (and other basins not shown here), we can conclude that up to d/o 60, no post-processing is indeed required for the Bender-type solutions. Beyond this wavelength range, however, a post-processing may be demanded to remove associating aliasing errors that would contaminate the Bender-type solutions. The smoothing kernel, which is needed to be applied for reducing the high frequency noise of Bender-type solutions is relatively smaller than the one required for GRACE products. The full error covariance matrices, e.g., estimated in Fig. 3, also suggest that the Bender-derived errors exhibit less correlated errors. As a result, an isotropic filter with small radius e.g, a Gaussian filter (Jekeli, 1981) with half width of 100-200 km might be sufficient for filtering future products of a Bender-type mission. More research requires for designing an optimum filter for the products of a Bender-type mission, which will be subjected to our further research.

Figure 6

Figure 7

Figure 8

Figure 9

4. Conclusion

In this study, one year recovery of monthly total water storage (TWS) signals using simulated observations from a Bender-type configuration was compared with that of GRACE-type simulations. Firstly, we have examined the recovery of TWS from both configurations under the instrumental noise and aliasing errors in different wavelength ranges of gravity field. According to this assessment, the test computations of the Bender-type simulations showed improvement up to spherical harmonics d/o 60 in detection of the 'global' water storage signal, especially in medium (d/o 80) and medium-to-short wavelength (d/o 100) harmonics with compared to the GRACE solutions, which showed an improvement up to spherical harmonics d/o 30 in 'global' TWS recovery.

Both TWS recovery scenarios with instrument noise-only, as well as that with instrument noise in the presence of aliasing errors (noise+aliasing errors), indicated that the aliasing errors contaminate the satellite gravimetry-derived TWS recovery and have to be seen as the dominant source of error.

Our performed comparisons between the recovered solutions determined by the Bender-type and GRACE formations and the simulated TWS signal from the global outputs of WGHM has been performed on a regional scale over the 33 world major river basins. Our results promised more detailed recovery of water storage changes from a Bender-type future gravity mission. Regarding the regional monthly recovery, the Bender-type constellation was able to detect about 90% of mass variations over some large and medium size river basins. Examples on the spatial domain have demonstrated such improvement from the Bender-type mission, when compared to the results of the GRACE formation.

Indeed, changing the spatial sampling (with keeping the temporal sampling as identical as real GRACE mission) via the Bender-type configuration could enhance the recovery of temporal mass changes in hydrology, detect the signal very well and reduce the temporal aliasing errors. Despite the importance of improving the temporal resolution issue, we find that maintaining the orbital period at 30 days repeating would provide sufficient spatial sampling, especially at equators of $\pm 60°$, where important temporal signals (e.g. hydrology and ocean) are taking place as recommended by the most recent ESA studies (NGGM Team, 2011, NG2 Team, 2011). However, it would be desirable in the future to improve the quality in detecting the temporal signal over certain areas in both spatial and temporal resolution together. This would be done by selecting shorter orbital repeating mode. To do this, a running of numerous simulation scenarios is required, which will be a subject of future consideration.

Aknowledgement

References

Awange, J. L., Fleming, K. M., Kuhn, M., Featherstone, W. E., Heck, B., Anjasmara, I. (2011) On the suitability of the 4° × 4° GRACE mascon solutions for remote sensing Australian hydrology. Remote Sensing of Environment, 115, 864–875. http://dx.doi.org/10.1016/j.rse.2010.11.014.

Awange, J., Forootan, E., Kusche, J., Kiema, J. K. B., Omondi, P., Heck, B., et al. (2013) Understanding the decline of water storage across the Ramser-Lake Naivasha using satellite-based methods. Advances in Water Resources, 60, 7–23. http://dx.doi.org/10.1016/j.advwatres.2013.07.002.

Bender, P. , Wiese, D., Nerem, R. (2008) A possible dual-GRACE mission with 90 degree and 63 degree inclination orbits, paper presented at Third International Symposium on Formation Flying, Eur. Space Agency, Noordwijk, Netherlands, 23–25 April.

Dahle, Ch., Frank, F., Gruber, Ch., König, D., König, R., Michalak, G., Neumayer, K-H. (2013) GFZ GRACE Level-2 Processing Standards Document for Level-2 Product Release 0005, (Scientific Technical Report STR12/02 – Data, Revised Edition, January 2013), Potsdam, 21 p. DOI: 10.2312/GFZ.b103-1202-25.

Döll, P., Kaspar, F., Lehner, B. (2003) A global hydrological model for deriving water availability indicators: model tuning and validation. Journal of Hydrology, Vol. 270:105134.

Eicker, A., Schumacher, M., Kusche, J., Döll, P., Müller Schmied, H. (2014) Calibration/data assimilation approach for integrating GRACE data into the WaterGAP Global Hydrology Model (WGHM) using an ensemble Kalman filter. Surveys in Geophysics, submitted.

Elsaka, B. (2010) Simulated Satellite Formation Flights for Detecting the Temporal Variations of the Earth's Gravity Field. Ph.D. Dissertation, University of Bonn, Germany.

Elsaka, B. (2014a) Sub-month Gravity Field Recovery from Simulated Multi-GRACE Mission Type. Acta Geophysica, Volume 62, Issue no. 1, Feb. 2014, pp 241-258, doi:10.2478/s-11600-013-0170-9.

Elsaka, B. (2014b) Feasible Multiple Satellite Mission Scenarios Flying in a Constellation for Refinement of the Gravity Field Recovery. International Journal of Geosciences, 5, 267-273. http://dx.doi.org/10.4236/ijg.2014.53027

Elsaka, B., Kusche, J., Ilk, K.-H. (2012) Recovery of the Earth's gravity field from formation-flying satellites: Temporal aliasing issues. Advances in Space Research, 50: 1534-1552. doi.org/10.1016/j.asr.2012.07.016.

Elsaka, B., Raimondo, J.-C, Brieden, Ph., Reubelt, T., Kusche, J., Flechtner, F., Iran Pour, S., Sneeuw, N., Müller, J. (2014) Comparing seven candidate mission configurations for temporal gravity retrieval through full-scale numerical simulation. . Journal of Geodesy. Vol. 88, No. 1. pp. 31-43. Doi. 10.1007/s00190-013-0665-9.

Fenoglio-Marc, L., Kusche, J., Becker, M. (2006) Mass variation in the Mediterranean Sea from GRACE and its validation by altimetry, steric and hydrologic fields. Geophys. Res. Lett. 33 (19) (2006). Doi.org/10.1029/2006GL026851.

Fenoglio-Marc, L., Rietbroek, R., Grayek, S., Becker, M., Kusche, J., Stanev, E. (2012) Water mass variation in the Mediterranean and Black Sea. Journal of Geodynamics, 59–60 (2012), pp. 168–182 http://dx.doi.org/10.1016/j.jog.2012.04.001.

Flechtner, F. (2007) AOD1b product description document for product releases 01 to 04, GRACE 327–750, GeoForschungszentrum Potsdam, Potsdam, Germany.

Flechtner, F., Thomas, M., Dobslaw, H. (2010) Improved non-tidal atmospheric and oceanic de-aliasing for GRACE and SLR satellites, Adv. Technol. Earth Sci., Part 2, 2010, 131–142, doi:10.1007/978-3-642-10228-8_11.

Flechtner, F., Morton, P., Watkins, M., Webb, F. (2014) Status of the GRACE Follow-on Mission, accepted for Proceedings of the International Association of Geodesy Symposia Gravity, Geoid and Height System, 09.-11.10.2012, Venice, Italy, IAGS-D-12-00141.

Förste, C., Schmidt, R., Stubenvoll, R., Flechtner, F., Meyer, U., Koenig, R., Neu-mayer, H., Biancale, R., Lemoine, J., Bruinsma, S., Loyer, S., Barthelmes, F., Esselborn, S. (2008) The GeoForschungsZentrum Potsdam/Groupe de Recherche de Ge-odesie Spatiale satellite-only and combined gravity field models: EIGEN-GL04S1 and EIGEN-GL04C. J Geod, 82, 6, 331-346, doi:10.1007/s00190-007-0183-8.

Forootan, E., Didova, O., Kusche, J., Löcher, A. (2013) Comparisons of atmospheric data and reduction methods for the analysis of satellite gravimetry observations. JGR-Solid Earth (2013) http://dx.doi.org/10.1002/jgrb.50160.

Forootan, E., Didova, O., Schumacher, M., Kusche, J., Elsaka, B. (2014a) Comparisons of atmospheric mass variations derived from ECMWF reanalysis and operational fields, over 2003 to 2011. Journal of Geodesy, in-press, doi: 10.1007/s00190-014-0696-x.

Forootan, E., Rietbroek, R., Kusche, J., Sharifi, M.A., Awange, J., Schmidt, M., Omondi, P., Famiglietti, J. (2014b) Separation of large scale water storage patterns over Iran using GRACE, altimetry and hydrological data. Journal of Remote Sensing of Environment, 140, Pages 580-595,dx.doi.org/10.1016/j.rse.2013.09.025

Frommknecht, B., Fackler, U., Flury, J., (2006) Integrated Sensor Analysis GRACE. Observation of the Earth System from Space, pp. 99–113, doi:10.1007/3-540-29522-4_8.

Han, S.-C., Jekeli, C., Shum, C.-K. (2004) Time-variable aliasing effects of ocean tides, atmosphere, and continental water mass on monthly mean GRACE gravity field, J. Geophys. Res., 109, B04403,doi:10.1029/2003JB002501.

Han, S. C., and Ditmar, P. (2008) Localized spectral analysis of global satellite gravity fields for recovering time-variable mass redistributions, J. Geod., 82, 423–430, doi:10.1007/s00190-007-0194-5.

Houborg, R., Rodell, M., Li, B., Reichle, R., Zaitchik, B. (2012) Drought indicators based on model assimilated GRACE terrestrial water storage observations, Wat. Resour. Res., 48, W07525, doi:10.1029/2011WR011291.

Iran Pour, S., Reubelt, T., Sneeuw, N. (2013) Quality assessment of sub-Nyquist recovery from future gravity satellite missions. Journal of Advances in Space Research Volume 52, Issue 5, Pages 916–929.

Jekeli, C. (1981) Alternative methods to smooth the Earth's gravity field. Rep. 327, Dept. of Geod. Sci. and Surv., Ohio State Univ., Columbus

Jensen, L., Rietbroek, R., Kusche, J. (2013) Land water contribution to sea level from GRACE and Jason-1 measurements, J. Geophys. Res. Oceans, 118, 212–226, doi:10.1002/jgrc.20058.

Kaula, W. M. (1967) Geophysical implications of satellite determinations of the Earth's gravitational field. Space Sci Rev 7: 769–794.

Kim, J. R. (2000) Simulation study of a low-low satellite-to-satellite tracking mission, PhD dissertation, University of Texas, Austin, Texas.

Klees, R., Zapreeva, E. A.,Winsemius, H. C., Savenije, H. H. G. (2007) The bias in GRACE estimates of continentalwater storage variations. Hydrology and Earth SystemSciences Discussions, 11, 1227–1241.

Klees, R., Revtova, E., Gunter, B., Ditmar, P., Oudman, E., Winsemius, H., Savenije, H. (2008) The design of an optimal filter for monthly GRACE gravity models, Geophys. J. Int., 175, 417–432,doi:10.1111/j.1365-246X.2008.03922.x.

Kurtenbach, E., Mayer-Gürr, T., Eicker, A. (2009) Deriving daily snapshots of the Earth's gravity field from GRACE L1B data using Kalman filtering. Geophysical Research Letters, Vol. 36, L17102, doi:10.1029/2009GL039564, 2009.

Kurtenbach, E., Eicker, A., Mayer-Gürr, T., Holschneider, M., Hayn, M., Fuhrmann, M., Kusche, J. (2011) Improved daily GRACE gravity field solutions using a Kalman smoother. Journal of Geodynamics, 59– 60 (2012) 39– 48.

Kusche, J. (2007) Approximate decorrelation and non-isotropic smoothing of time-variable GRACE-type gravity field models. Journal of Geodesy, Vol. 81:733-749.

Kusche, J., Schmidt, R., Petrovic, S., Rietbroek, R. (2009) Decorrelated GRACE time-variable gravity solutions by GFZ, and their validation using a hydrological model. Journal of Geodesy, Vol. 83. pp. 903-913.

Kusche, J., Eicker, A., Forootan, E. (2011) Analysis tools for GRACE and related data sets, theoretical basis. The International Geoscience Programme (IGCP). IGCP 565: Supporting water

resource management with improved Earth observations.
www.igcp565.org/workshops/Johannesburg_2011/kusche_LectureNotes_analysistools.pdf

Kusche, J., Klemann, V., Bosch, W. (2012) Mass distribution and mass transport in
the Earth system. Journal of Geodynamics, 59–60, 1–8. http://dx.doi.org/10.1016/
j.jog.2012.03.003.

Longuevergne, L., Scanlon, B., Wilson, C. (2010) GRACE Hydrological estimates for small
basins: Evaluating processing approaches on the High Plains Aquifer, USA. Water Resources
Research, 46 (11) (2010), p. W11517 http://dx.doi.org/10.1029/2009WR008564.

Mayer-Gürr, T., Kurtenbach, E., Eicker, A. (2010) ITG-Grace2010 gravity field model. URL:
www.igg.uni-bonn.de/apmg/index.php.

NG2 Team (2011): Rathke, A. et al. (2011) Assessment of a Next Generation Gravity Mission
to Monitor the Variations of Earth's Gravity Field. Final Report, ESTEC Contract No.:
22672/09/NL/AF. Doc. No.: NG2-ASG-FR, Issue 1, 10 Oct. 2011.

**NGGM Team (2011): Anselmi, A., Cesare, S., Visser, P., Van Dam, T., Sneeuw, N., Gruber,
T., Altes, B., Christophe, B., Cossu, F., Ditmar, P. Murboeck, M., Parisch, M., Renard, M.,
Reubelt, T., Sechi, G., Texieira Da Encarnacao, JG. (2011)** Assessment of a next generation
gravity mission to monitor the variations of Earth's gravity field. ESA Contract No.
22643/09/NL/AF, Executive Summary, Thales Alenia Space report SD-RP-AI-0721, March
2011.

Pierce, R., Leitch, J., Stephens, M., Bender, P., Nerem, R. (2008) Inter-satellite range
monitoring using optical interferometry, Appl. Optics, 47 (27),5007–5019, doi:10.1364/AO.47.00
5007.

Rodell, M., Houser, P., Jambor, U., Gottschalck, J., Mitchell, K., Meng, K. (2004) The global
land data assimilation system. Bulletin of the American Meteorological Society, 85 (3), pp. 381–
394.

Savcenko, R. and Bosch, W. (2008) EOT08a – empirical ocean tide model from multi-mission
satellite altimetry. Report No. 81, Deutsches Geodätisches Forschung-sinstitut (DGFI), München.

Savcenko, R. and Bosch, W. (2012) EOT11a – empirical ocean tide model from multi-mission
satellite altimetry. Report No. 89, Deutsches Geodätisches Forschung-sinstitut (DGFI), München.

Schmidt, M., Seitz, F., Shum, C.-K. (2008) Regional four-dimensional hydrological mass
variations from GRACE, atmospheric flux convergence, and river gauge data. Journal of
Geophysical Research, 113 (2008), p. B10402. doi.org/10.1029/2008JB005575.

Schumacher, M., Eicker, A., Kusche, J., Müller-Schmied, H., Döll, P. (2014). Covariance Analysis and Sensitivity Studies for GRACE Assimilation into WGHM, IAG Scientific Assembly Proceedings. In-press.

Sharifi, M., Sneeuw, N., and Keller, W. (2007) Gravity Recovery capability of four generic satellite formations. In Proc. Kilicoglu, A. and R. forsberg (Eds.), Gravity Field of the Earth. General Command of Mapping, ISSN 1300-5790, Special issue 18, 211–216.

Sheard, B., Heinzel, G., Danzmann, K., Shaddock, D., Klipstein, W., Folkner, W. (2012) Intersatellite laser ranging instrument for the GRACE follow-on mission. Journal of Geodesy, Vol. 86, Number 12, Page 1083.

Sneeuw, N., Flury, J., Rummel, R. (2004) Science requirements on future missions and simulated mission scenarios, Earth, Moon, and Planets, 94, 113–142, doi:10.1007/s11038-004-7605-X.

Sneeuw, N., Sharifi, M., and Keller, W. (2008) Gravity Recovery from Formation Flight Missions. Xu, Peiliang, Jingnan Liu and Athanasios Dermanis (Eds.), VI Hotine-Marussi Symposium on Theoretical and Computational Geodesy, Vol. 132, Springer, Berlin Heidelberg, 29–34.

Swenson, S., and Wahr, J. (2002) Estimated effects of the vertical structure of atmospheric mass on the time-variable geoid, J. Geophys. Res., 107(9), 2194, doi:10.1029/2000JB000024.

Swenson, S., and Wahr, J. (2006) Post-processing removal of correlated errors in GRACE data, Geophys. Res. Lett., 33, L08402, doi:10.1029/ 2005GL025285.

Tapley, B., Bettadpur, S., Ries, J. C., Thompson, P., Watkins, M. (2004) GRACE measurements of mass variability in the Earth system, Science, 305, 503–505, doi:10.1126/science.1099192.

Tapley, B., Ries, J., Bettadpur, S., Chambers, D., Cheng, M., Condi, F., Gunter, B., Kang, Z., Nagel, P., Pastor, R., Pekker, T., Poole, S., Wang, F. (2005) GGM02 – An improved Earth gravity field model from GRACE. J Geod (2005) 79: 467–478.

Thales Alenia Space, (2008) Laser Interferometry High Precision Tracking for LEO, Summary Report, SD-RP-AI-0584, September 2008.

Visser, P., Sneeuw, N., Reubelt, T., Losch, M., van Dam, T. (2010) Space-borne gravimetric satellite constellations and ocean tides: aliasing effects. Geophys. J. Int. (2010) 181, 789–805.

Wiese, D., Folkner, W. and Nerem, R. (2009) Alternative mission architectures for a gravity recovery satellite mission. Journal of Geodesy, 83, 569-581, DOI 10.1007/s00, 190-008-0274-1.

Wiese, D., Nerem, R., Han, S.-C. (2011) Expected improvements in determining continental hydrology, ice mass variations, ocean bottom pressure signals, and earthquakes using two pairs of

dedicated satellites for temporal gravity recovery. Journal of Geophysical Research, Vol. 116, B11 405, doi:10.1029/2011JB008375.

Wiese, D., Nerem, R., Lemoine, F. (2012) Design considerations for a dedicated gravity recovery satellite mission consisting of two pairs of satellites. Journal of Geodesy, 86:81-98, DOI 10.1007/s00190-011-0493-8.
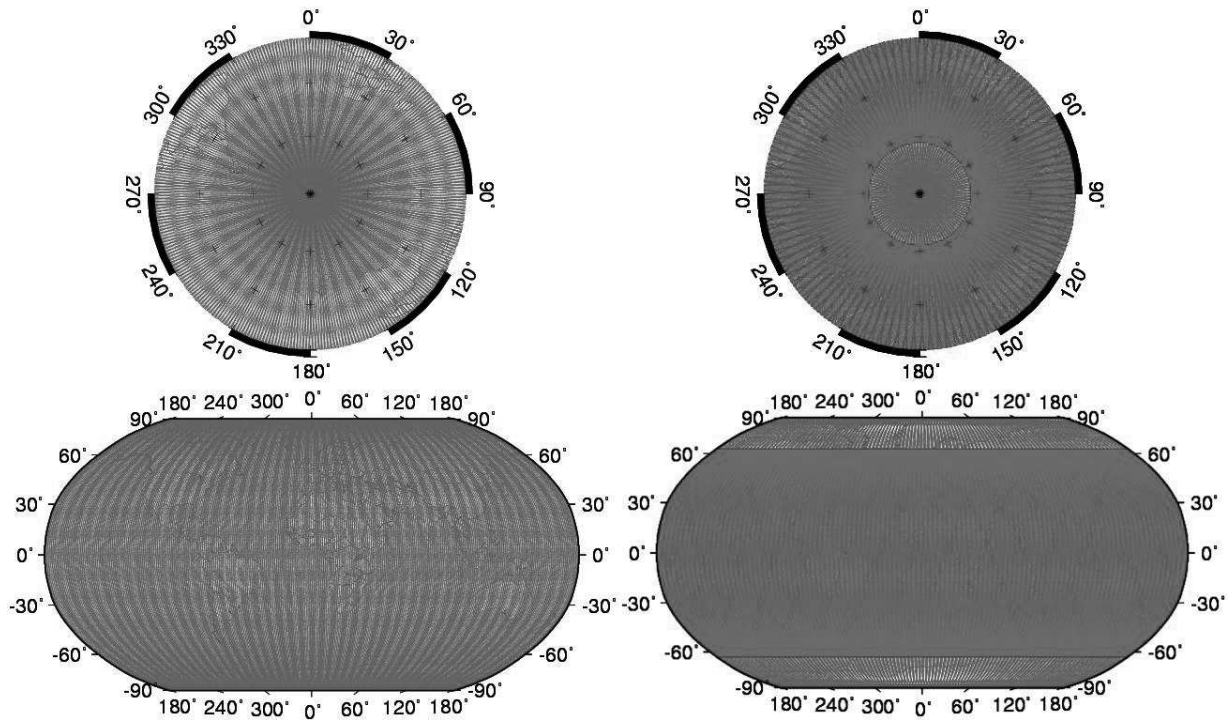
Fig.1: Satellite ground-tracks of GRACE (left) and Bender-type (right) satellite configurations from polar (top) and equatorial (bottom) views.

Table 1. Background models used for the numerical simulation.

Models	Orbit integration	Gravity analysis (noise-only)	Gravity analysis (noise + aliasing)
mean gravity field	ITG-GRACE2010s (Mayer-Gürr et al., 2010b)	Same	Same
Atmosphere and ocean	100% of AOD-1B (Flechtner, 2007)	Same	90% of AOD-1B
ocean tides	EOT08a (Savcenko and Bosch 2008)	same	EOT11a (Savcenko and Bosch 2012)
Hydrology	WGHM (Döll et al. 2003)	None	None
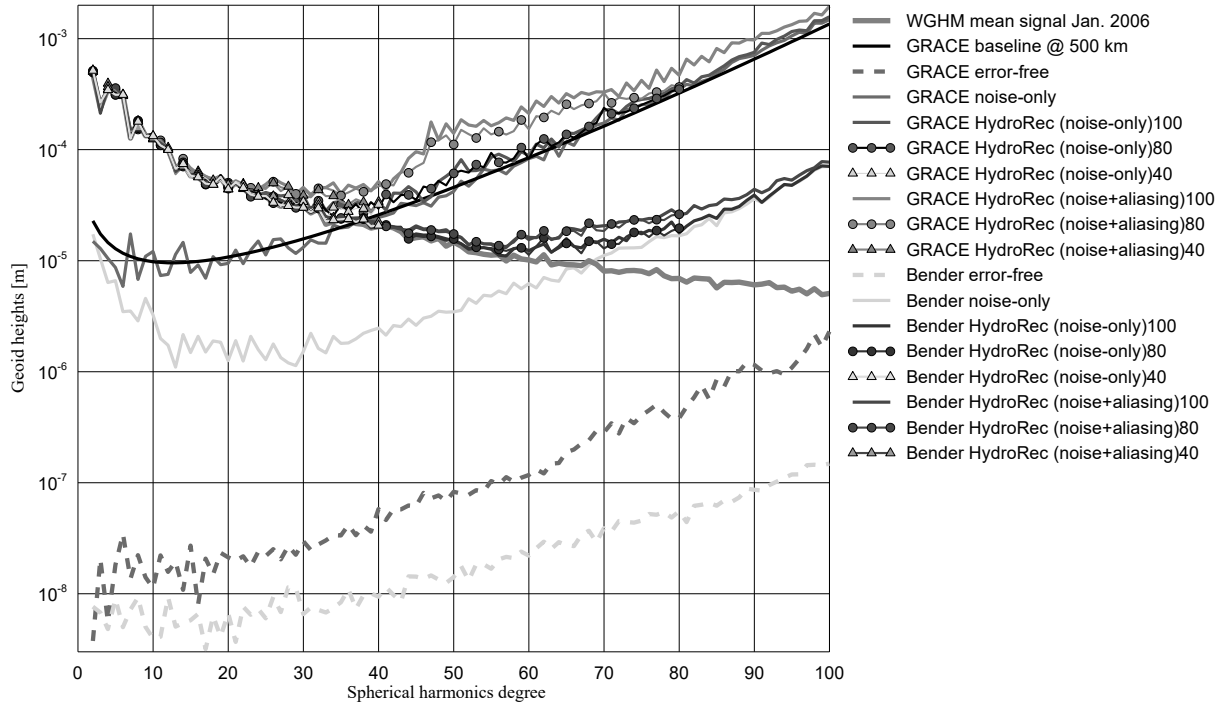
Fig. 2: Difference degree variances in terms of geoid heights [m] in recovering the introduced monthly TWS fields at different SHDs of 40, 80 and 100.
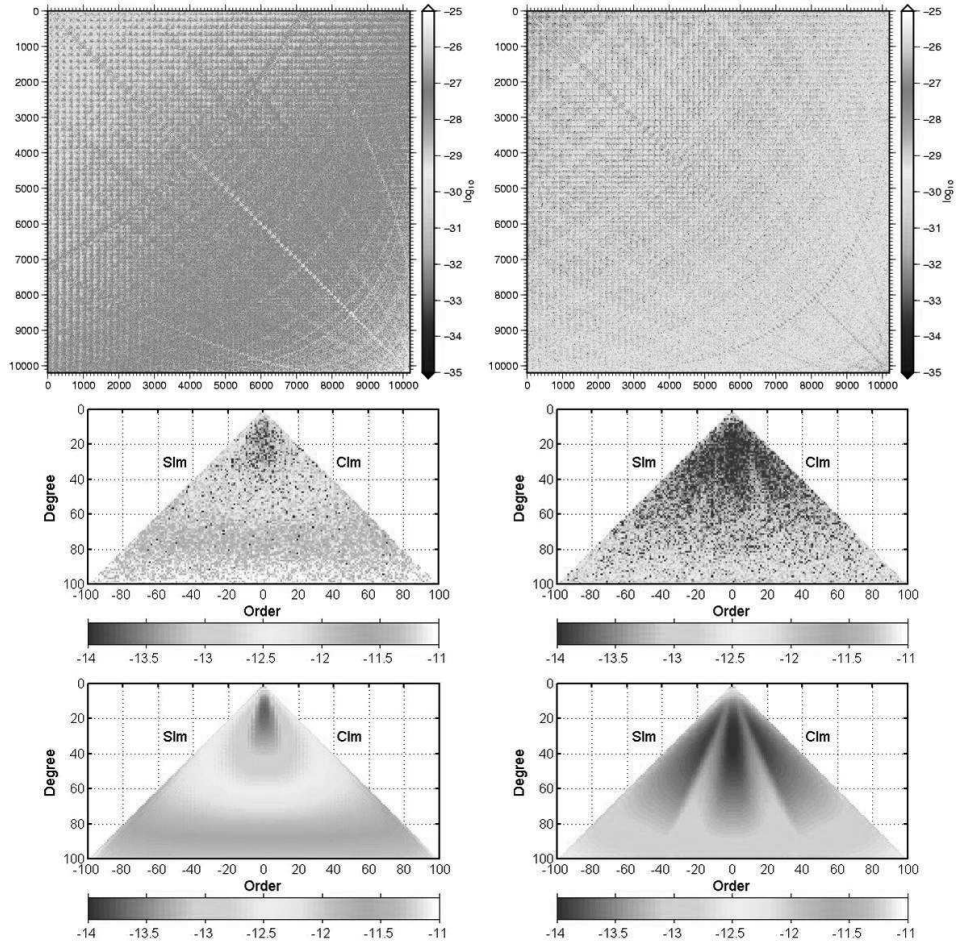
Fig. 3: Full error information from covariance matrix (top), degree variances (middle) and formal errors (bottom) of the GRACE (left) and Bender-type (right) gravity 'noise-only' solutions.

Table 2. Global RMS values in terms of geoid heights [mm] for both GRACE and Bender-type configurations considering noise-only and noise + aliasing errors cases given in Fig. 2.

Scenario / Mission	Water Storage Recovery RMS (mm), noise-only			Water Storage Recovery RMS (mm), noise + aliasing errors		
	d/o 40	d/o 80	d/o 100	d/o 40	d/o 80	d/o 100
GRACE	0.902	1.41	4.83	0.933	1.77	6.24
Bender	0.901	0.910	0.935	0.907	0.918	0.955
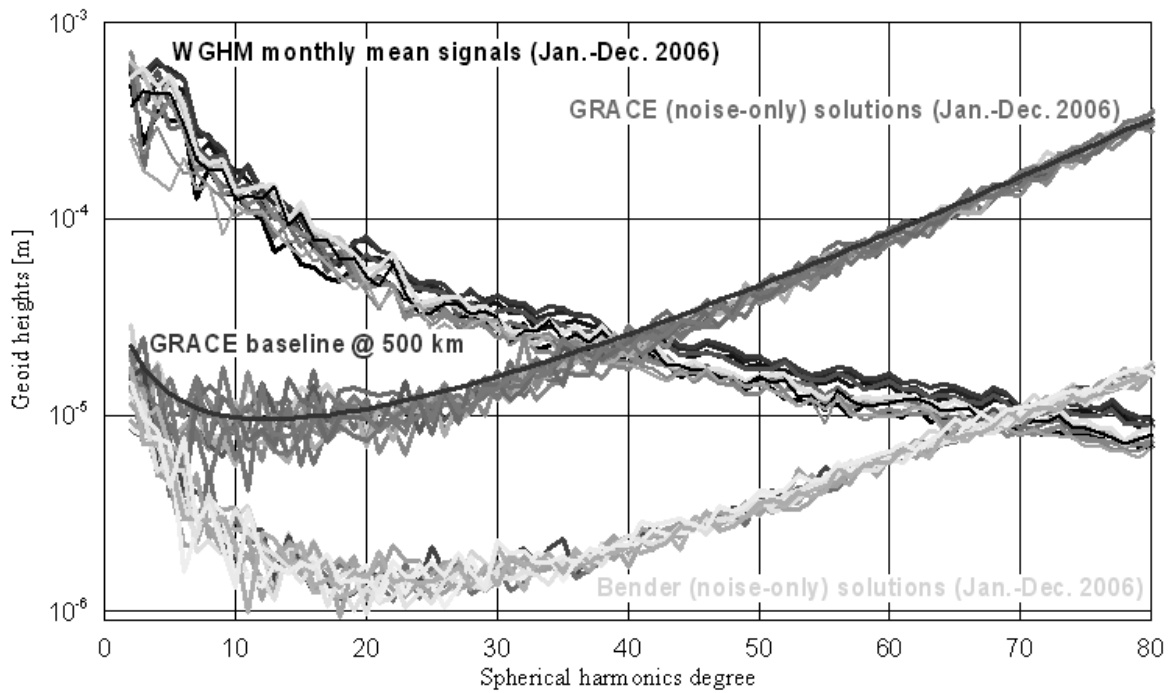
Fig. 4: Gravity field solutions determined by the GRACE (red curves) and Bender-type (green curves) configurations considering noise-only case.
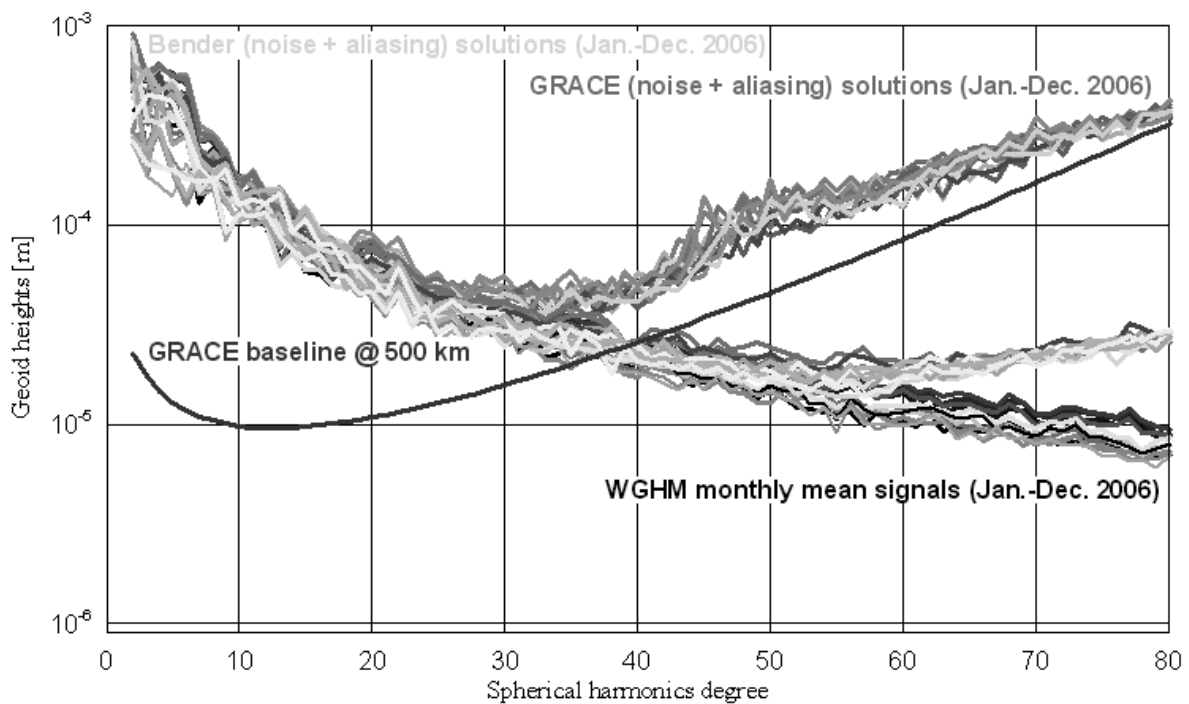
Fig. 5: Monthly gravity field solutions in terms of hydrology recovery determined by the GRACE (red curves) and Bender-type (green curves) configurations considering noise + aliasing case.
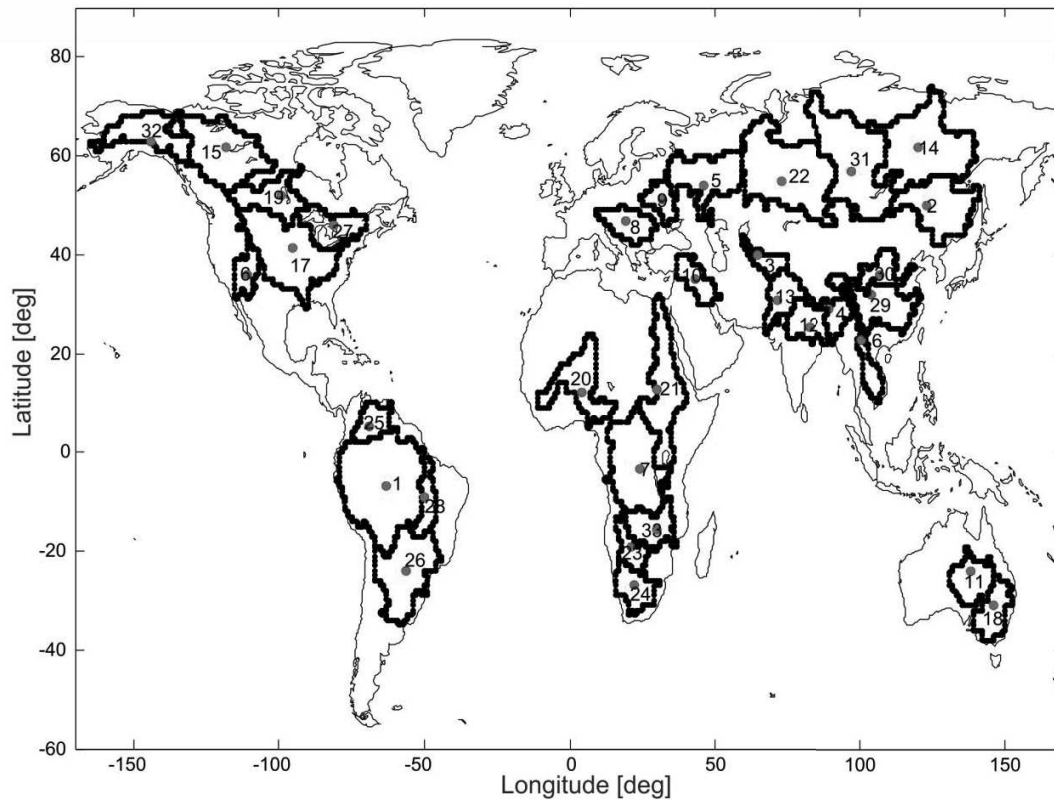
1- Amazon, 2- Amur, 3-Amu Darya, 4- Brahmaputra, 5- Volga, 6- Colorado (Arizona), 7- Congo, 8- Danube
9- Dnieper, 10- Euphrates, 11- Eyrie, 12- Ganges, 13- Indus, 14-Lena, 15- Mackenzie, 16- Mekong, 17- Mississippi
18- Murray, 19- Nelson, 20- Niger, 21- Nile, 22- Ob, 23- Okavango, 24- Orange, 25- Orinoco, 26- Parana,
27- St. Lawrence, 28- Tocantins, 29- Yangtze, 30- Yellow, 31- Yenisey, 32- Yukon, and 33- Zambezi.

Fig. 6 Geographical distribution of the investigated world's 33 major river basins. The red dots represent the middle latitude and longitude of the basins. The position of the middle points is given for each basin in Figure 7.

(7a)

(7b)

28
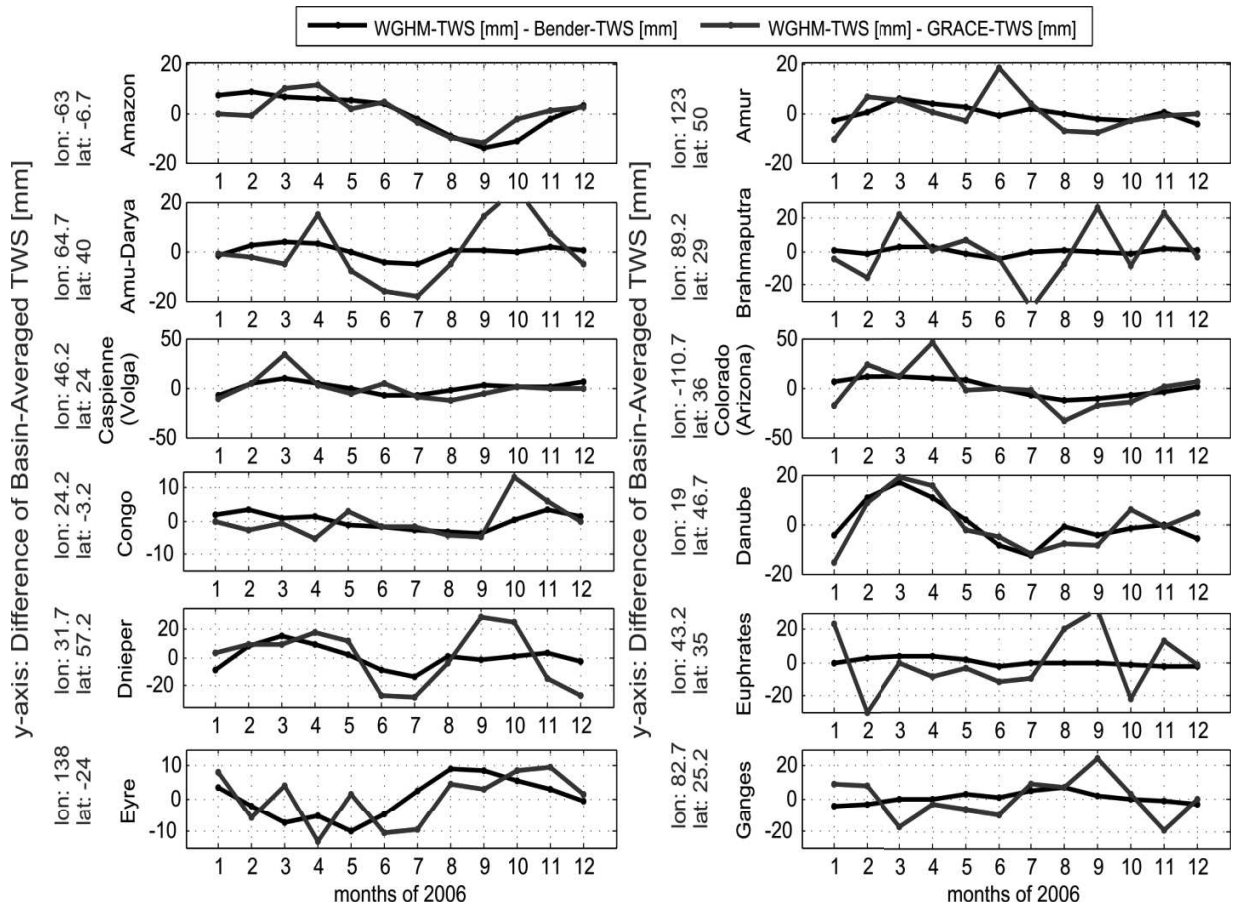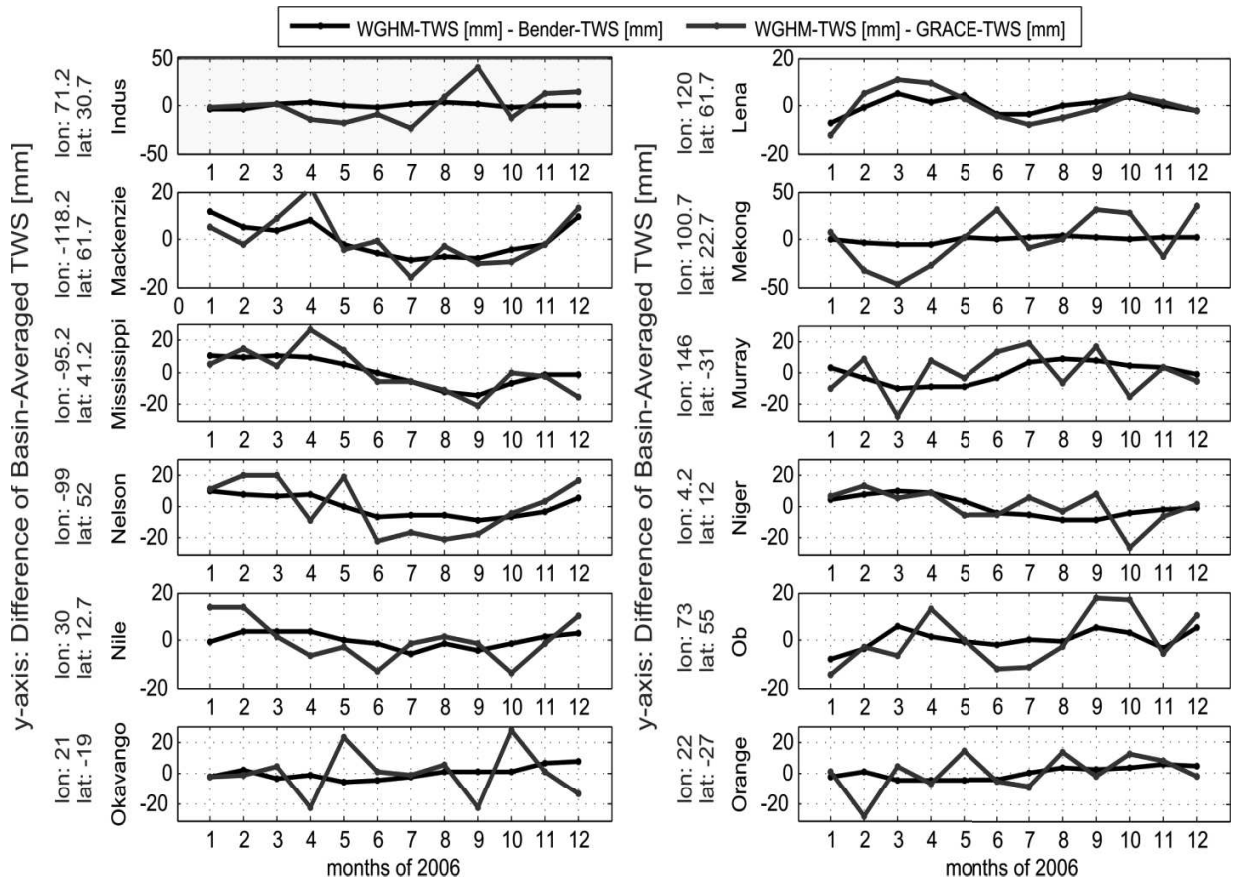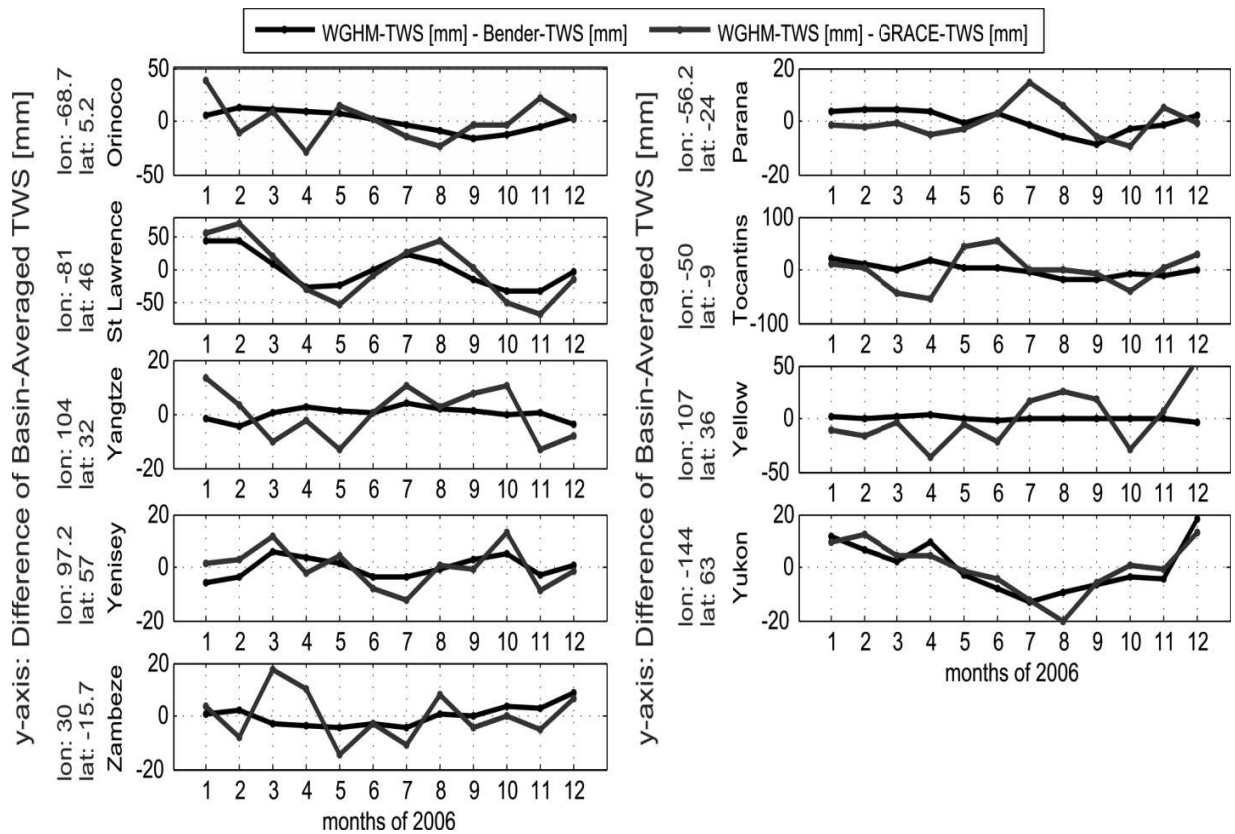
(7c)

Fig. 7 Mass variations in total water storage for 33 basins (7a, 7b and 7c). The graphs show the difference between recovered water storage changes determined by the Bender-type and GRACE-like configurations and the original TWS signal of WGHM. The x axis stands for months and y axis stands for the equivalent water height in [mm].

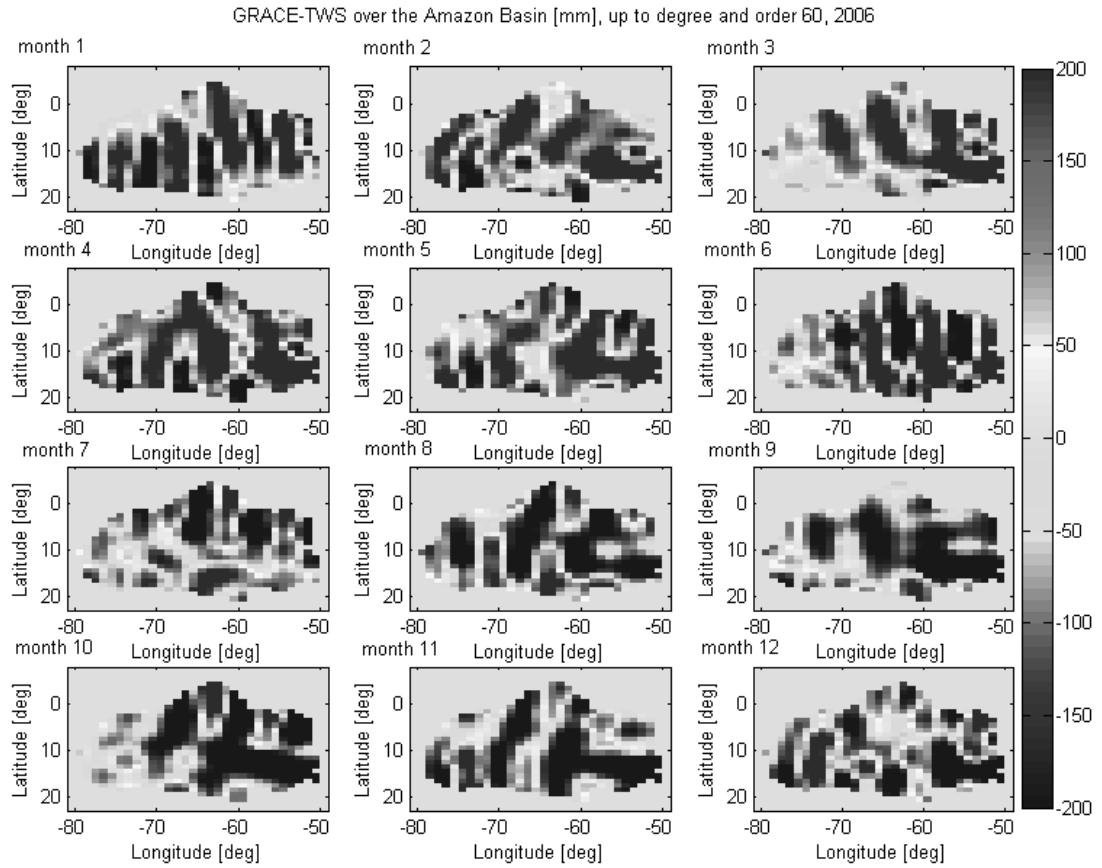WGHM-TWS over the Amazon Basin [mm], up to degree and order 60, 2006
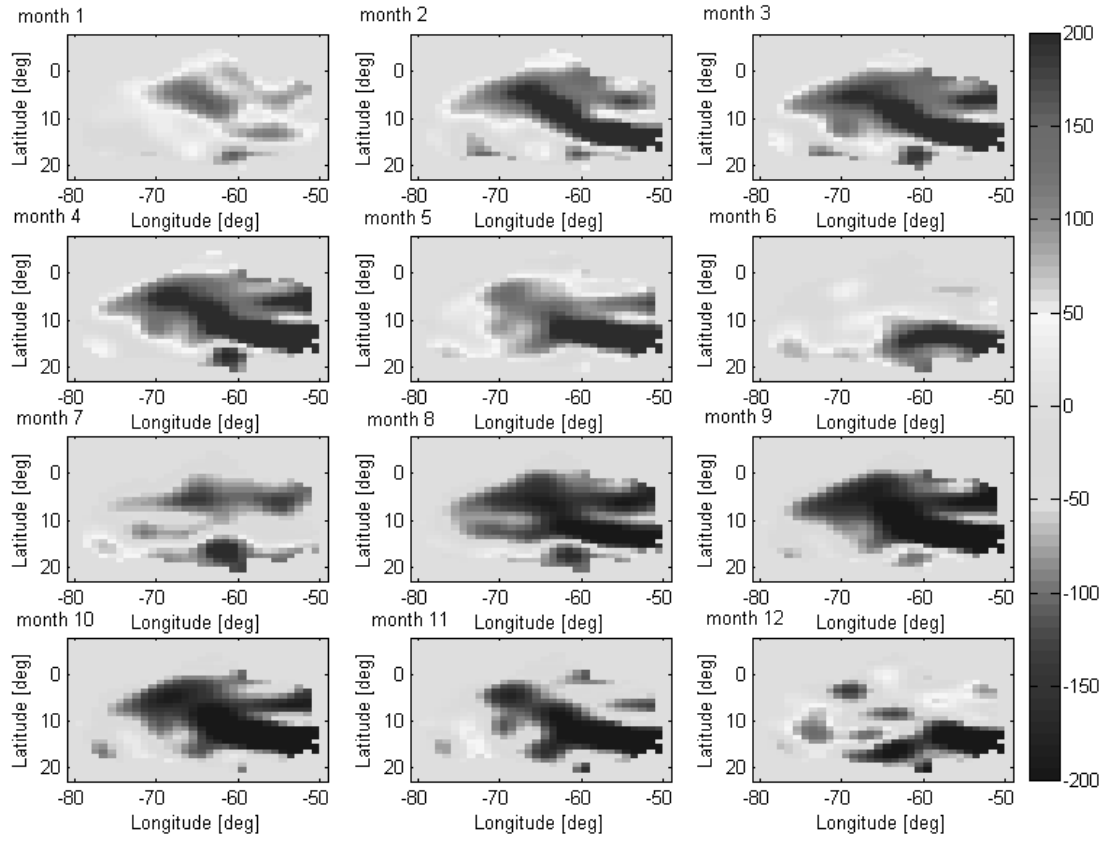
(7a)

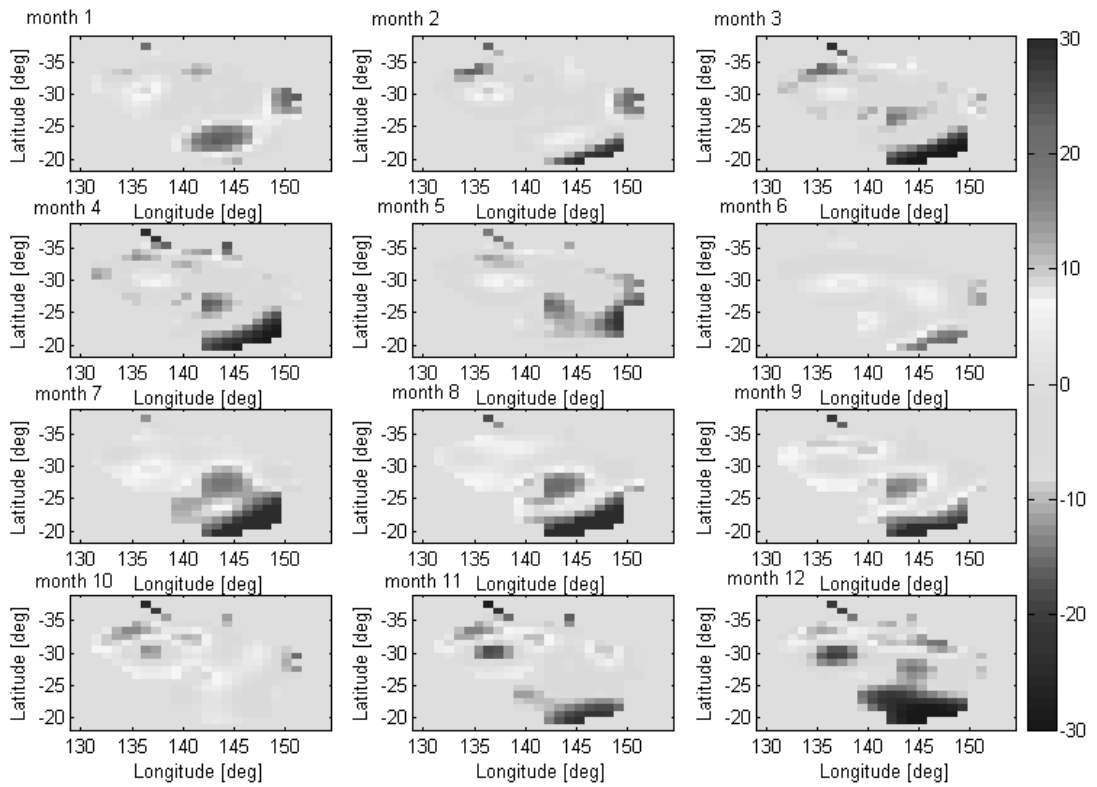Bender-TWS over the Amazon Basin [mm], up to degree and order 60, 2006

(7b)

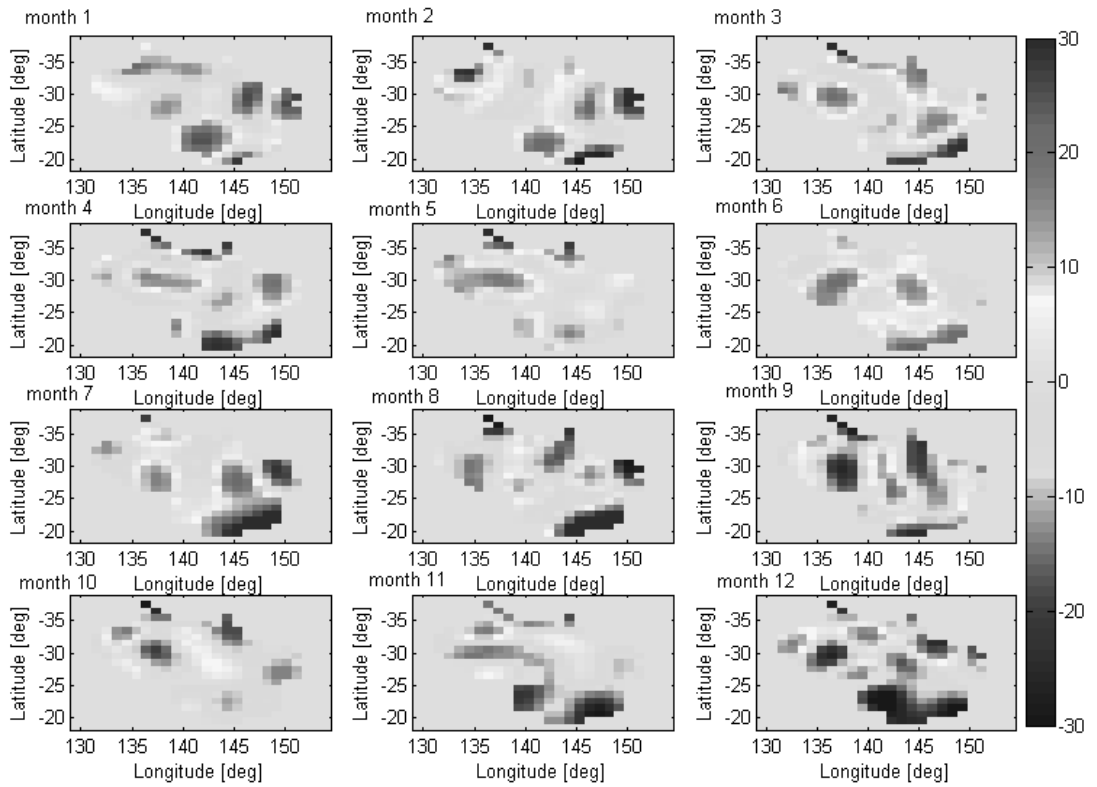GRACE-TWS over the Amazon Basin [mm], up to degree and order 60, 2006
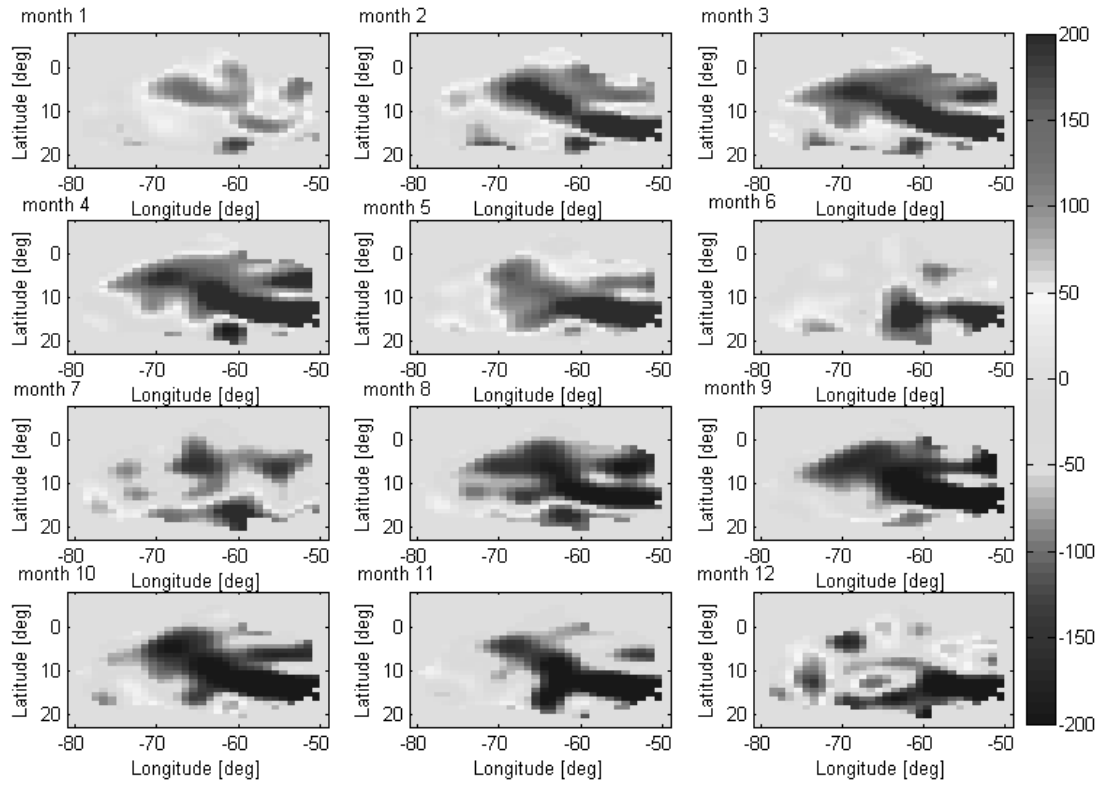
(8c)

Fig. 8 Mass variations in total water storage in terms of equivalent water height in [mm] for the Amazon basin as determined by the Bender-type (8b) and GRACE (8c) compared with the original signal of WGHM (8a). The x and y axes stand for longitude and latitude in degrees, respectively.

WGHM-TWS over the Eyre and Murrary Basins [mm], up to degree and order 60, 2006
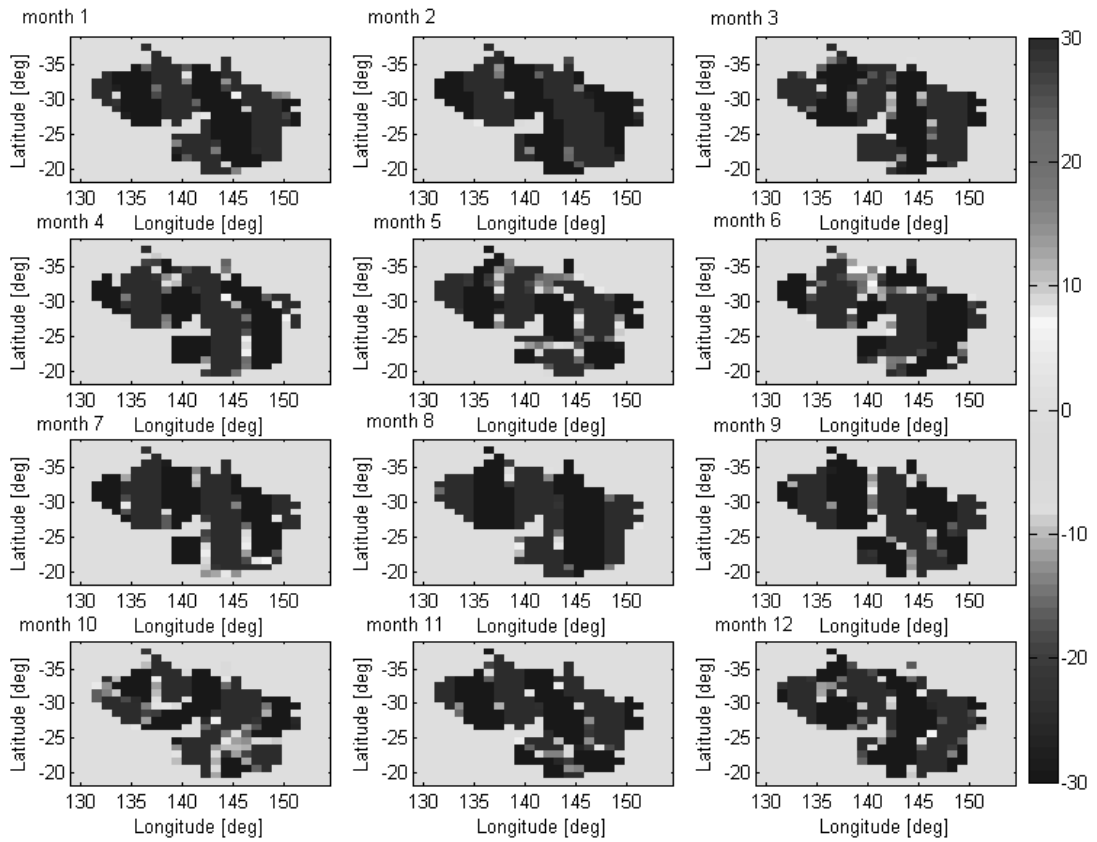
(9a)

Bender-TWS over the Eyre and Murrary Basins [mm], up to degree and order 60, 2006

(9b)

GRACE-TWS over the Eyre and Murrary Basins [mm], up to degree and order 60, 2006

(9c)

Fig. 9 Mass variations in total water storage in terms of equivalent water height in [mm] for the Murrary+Eyre basins as determined by the Bender-type (9b) and GRACE (9b) compared with the original signal of WGHM (9a). The x and y axes stand for longitude and latitude in degrees, respectively.